EPJ manuscript No.
(will be inserted by the editor)

Difference-frequency combs in cold atom physics

Russell Kliese[1], Nazanin Hoghooghi[1], Thomas Puppe[1,a], Felix Rohde[1], Alexander Sell[1], Armin Zach[1], Patrick Leisching[1], Wilhelm Kaenders[1], Niamh C. Keegan[2], Alistair D. Bounds[2], Elizabeth M. Bridge[2], Jack Leonard[1,2], Charles S. Adams[2], Simon L. Cornish[2], and Matthew P. A. Jones[2]

[1] TOPTICA Photonics AG, Lochhamer Schlag 19, 82166 Graefelfing, Germany
[2] Joint Quantum Centre (JQC) Durham-Newcastle, Department of Physics, Durham University, Durham DH1 3LE, UK

Abstract Optical frequency combs provide the clockwork to relate optical frequencies to radio frequencies. Hence, combs allow optical frequencies to be measured with respect to a radio frequency where the accuracy is limited only by the reference signal. In order to provide a stable link between the radio and optical frequencies, the two parameters of the frequency comb must be fixed: the carrier envelope offset frequency, f_{ceo}, and the pulse repetition-rate, f_{rep}. We have developed the first optical frequency comb based on difference frequency generation (DFG) that eliminates f_{ceo} by design — specifically tailored for applications in cold atom physics. An f_{ceo}-free spectrum at 1550 nm is generated from a super continuum spanning more than an optical octave. Established amplification and frequency conversion techniques based on reliable telecom fibre technology allow the generation of multiple wavelength outputs. The DFG comb is a convenient tool to both stabilise laser sources and accurately measure optical frequencies in Rydberg experiments and more generally in quantum optics. In this paper we discuss the frequency comb design, characterization, and optical frequency measurement of Strontium Rydberg states. The DFG technique allows for a compact and robust, passively f_{ceo} stable frequency comb significantly improving reliability in practical applications.

1 Introduction

An exact measurement of a frequency requires a clockwork to establish a phase coherent link between the frequency to be measured and a reference oscillator of known frequency. An optical frequency comb is an elegant solution providing such a clockwork between two optical frequencies or an optical and a microwave (RF) frequency [1,2]. It is hence an essential building block for practical implementations of optical clocks [3,4,5]. Other applications include precision measurements, generation of arbitrary optical frequencies and the transfer of optical and radio frequencies. Quantum

[a] e-mail: `thomas.puppe@toptica.com`

optics experiments require accurate measurement and stabilization of optical frequencies for preparation, precise control and probing of the quantum system. With cumulative sophistication of experimental schemes and required control, the light fields span increasingly large ranges in wavelength. For example in Rydberg experiments, in addition to the first excited states used for initial preparation, a number of higher excited levels are addressed. While it is possible to stabilise a laser on ground state transitions, e.g., with Doppler-free absorption spectroscopy, this becomes significantly more difficult for transitions to higher states. The frequency comb provides a universal method of accessing several arbitrary optical frequencies, all exactly referenced to a common reference oscillator. The comb therefore provides a convenient tool to both accurately stabilise laser sources and accurately measure optical frequencies in Rydberg experiments and more generally in quantum optics.

In this paper we provide practical insight into how a frequency comb with multiple outputs at different wavelengths based on difference frequency generation (DFG) proves to be a useful tool in Rydberg experiments. The DFG comb provides a simpler relationship between optical and RF frequencies than conventionally stabilised combs and is a robust tool owing to reduced electronic locking requirements.

The specific frequency comb described here was build by TOPTICA Photonics AG in collaboration with the atomic and molecular physics groups at Durham University. The goal was to develop a frequency comb with four separate measurement outputs, spanning the wavelength range 638 nm–1550 nm, to support experiments on high-precision spectroscopy of Strontium (Sr) Rydberg states [6] and ultracold Rubidium-Caesium (RbCs) molecules [7]. While DFG combs have been demonstrated previously, we present their application as an instrument to support complex multi-wavelength cold atom experiments. We find that using the DFG technique results in a highly stable comb that runs reliably with almost no optimisation by the end user. In this paper we review properties of frequency combs as a tool for quantum optics, discuss in detail the DFG comb and present precision spectroscopy of Sr Rydberg states as an example application.

2 How the frequency comb works

Optical frequency combs are typically based on passively mode-locked oscillators emitting a train of pulses separated by the round trip time of the optical resonator. The optical phases of the frequency components supported by the resonator are phase locked by the mode-lock mechanism to form short pulses. Mode-locked oscillators in frequency combs are commonly based on Ti:Sapphire (<10 fs) [8,9], as well as erbium doped fibre (< 100 fs) [10,11]. The pulse length is fundamentally Fourier-limited by the gain bandwidth. In the frequency domain the pulse train results in a spectrum of equidistant modes separated by the repetition rate, f_{rep} given by the inverse round-trip time, see Fig. 1. Due to the difference between phase and group velocities within the oscillator, the phase of the optical carrier shifts with respect to the pulse envelope from pulse-to-pulse. This gives rise to the carrier envelope phase shift which amounts to a non-zero frequency offset, f_{ceo}, in the Fourier spectrum. Hence the comb spectrum generated from a mode-locked short-pulse laser is completely defined by these two parameters. The frequency of the comb lines , ν_n, are given by:

$$\nu_n = n \times f_{\mathrm{rep}} + f_{\mathrm{ceo}}, \tag{1}$$

with $n \in \mathbb{N}$ denoting the comb tooth order.

The repetition rate is directly linked to the optical path length in the resonator and hence an actuator for the cavity length is the obvious choice to vary the repetition rate, e.g., through the use of a piezo actuator. The carrier envelope frequency

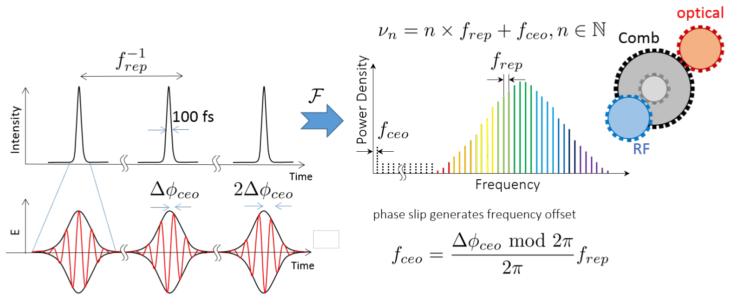

Figure 1. The optical frequency comb: A mode-locked short-pulse laser emits a train of equidistant short pulses. The Fourier spectrum ($\mathcal{F}$) is a comb of optical lines separated by the repetition rate, f_{rep}. Due to the mode-locking all lines have well defined relative optical phases. The carrier envelope offset frequency, f_{ceo}, represents the offset to zero frequency. It is given by the phase slip, ϕ_{ceo}, of the optical carrier with respect to the pulse envelope between consecutive pulses. The position of the comb lines in the frequency domain is completely defined by (f_{rep}, f_{ceo}) and therefore provides a clockwork to link optical and RF frequencies.

induced by a pulse-to-pulse phase shift, can be influenced by acting on group velocity dispersion in the oscillator, e.g., by pump current modulation [12]. Alternatively, f_{ceo} can be stabilised externally by a frequency actuator, e.g., an acousto-optical modulator (AOM) [13], which can also be implemented in a feed-forward scheme. A well-established scheme to measure f_{ceo} is an f–$2f$ interferometer, where f_{ceo} is detected via a beat between the frequency-doubled low frequency end (containing $2f_{\mathrm{ceo}}$ due to the frequency doubling process) and the high frequency end of an octave spanning spectrum [12]. In a difference-frequency comb, instead of detecting and stabilizing f_{ceo} in a feedback loop, it is fundamentally removed by DFG, leaving only a single parameter, f_{rep}, to be stabilised.

3 The difference frequency comb

DFG combs have previously been realised in pulsed Ti:Sapphire lasers to generate f_{ceo}-free spectra in the IR [14,15] as well as Ytterbium doped fibre combs. These DFG combs have the disadvantage that the resulting f_{ceo}-free spectra do not lie within the original gain medium. A technologically elegant solution, used for the DFG comb presented here, is based on a more than octave spanning super continuum such that the DFG output is at the original erbium oscillator spectrum at 1550 nm [16,17]. This allows reuse of the same frequency conversion techniques, based on reliable, mass-produced telecommunications fibre components, previously developed for erbium fibre oscillators.

Fig. 2 illustrates the process of generating the f_{ceo}-free comb from the spectrum of a fibre oscillator. First the spectrum is amplified and broadened in a highly nonlinear fibre (HNLF) to include 850 nm and 1880 nm spectral components. The difference frequency of these parts of the spectrum is subsequently generated in a periodically poled lithium niobate (PPLN) non-linear crystal. Details of the setup can be found in [16]. Since the comb teeth are coherent the difference of multiple combinations of lines $(n-m) \equiv \bar{n} = const.$ contribute to a single line in the DFG spectrum according to:

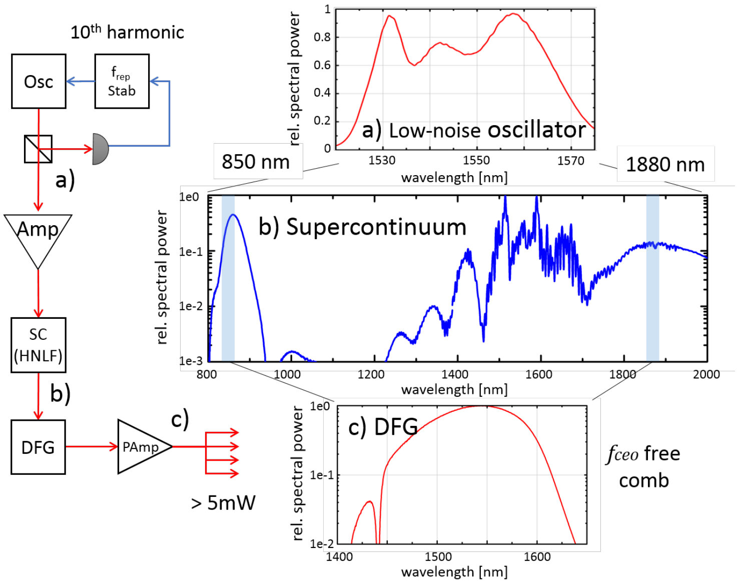

Figure 2. DFG comb: In a difference frequency comb (DFG-FC) the f_{ceo} is removed by mixing two parts of the spectrum. In this particular DFG-FC a super continuum spanning more than an optical octave (b) is generated from the low-noise oscillator (a) using a highly nonlinear fibre (HNLF). Difference frequency generation (DFG) between the ends at 850 nm and 1880 nm results in a passively f_{ceo}-stable output at 1550 nm (c). The f_{ceo}-free comb spectrum at 1550 nm can then be amplified and frequency converted with established techniques based on Er:fibre technology. The optical spectra of the low-noise oscillator, supercontinuum and DFG output are shown in relative spectral power on a linear and logarithmic scale, respectively

$$\underbrace{\nu_n - \nu_m}_{\nu_{\bar{n}}} = \underbrace{(n-m)}_{\bar{n}} \times f_{\text{rep}} + \underbrace{(f_{\text{ceo}} - f_{\text{ceo}})}_{\equiv 0} \quad (2)$$

$$\nu_{\bar{n}} = \bar{n} \times f_{\text{rep}}, \quad (3)$$

After the DFG the f_{ceo} is equal to zero and the comb lines are integer multiples of f_{rep} (eq. 3).

Due to the fundamental removal of f_{ceo} in the DFG process, the comb system can be significantly simplified. The DFG comb requires only a single active loop to stabilise f_{rep} and avoids problems associated with cross-talk between actuators that must be considered in non-DFG combs [18,19]. This simplification makes it easier to ensure the comb remains locked to the stable RF reference leading to a greater certainty that experimental results are accurate. A frequency comb that is stabilised can provide the basis for linking continuous-wave (cw) lasers. These can be locked to a precise absolute frequency or the comb can facilitate precise absolute frequency measurement.

4 Linking continuous-wave laser and frequency comb

There are two common ways a frequency comb is used alongside cw lasers for precision spectroscopy, both requiring identical hardware. The frequency comb can either be

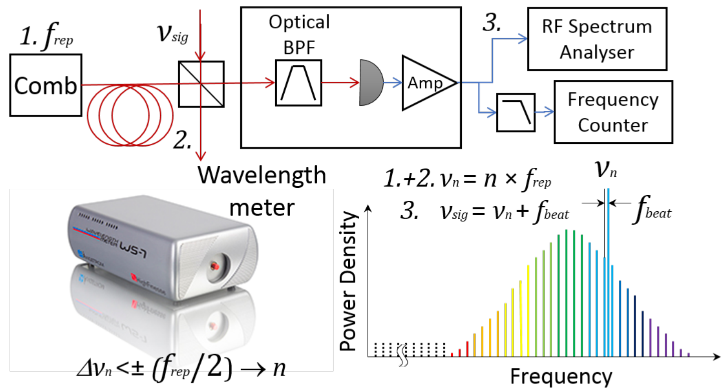

Figure 3. Measurement of the frequency of a continuous-wave (cw) laser with a difference frequency comb typically includes three steps: 1. measurement of the repetition frequency f_{rep}, 2. measurement of the cw laser frequency to within one f_{rep} to identify the order n of a nearby comb tooth, e.g., with a wavelength meter and 3. measurement of the beat between the laser and this comb tooth as an RF offset frequency. For locking the laser to the comb the beat offset frequency is phase locked. To improve the signal to noise ratio (SNR) of the beat, the relevant part of the comb spectrum is isolated by an optical bandpass filter (BPF) that reduces the optical power incident on the beat photo diode from the rest of the comb.

used as a reference for measuring an unknown frequency of a cw laser or a cw laser may be locked to the comb to provide a precisely defined cw laser frequency.

An unknown optical frequency of a cw laser can be measured by first locking the frequency comb to an RF reference. This is commonly achieved by detecting f_{rep} with a photo detector and acting on a piezo actuator, forming a phase-locked loop (PLL). This provides an absolutely stable frequency comb with precisely spaced comb lines separated by f_{rep} with an accuracy typically limited only by the performance of the RF reference. It is also possible to measure an unknown optical frequency without locking the frequency comb to a reference by precisely measuring f_{rep} and appropriate compensation in a *transfer method*, however, to simplify the explanations in this section, we assume that the frequency comb is locked to a stable reference.

The measurement of the unknown frequency of the cw laser is depicted in Figure 3 and consists of three steps. First, the repetition frequency f_{rep} is precisely measured with a counter or precisely known beforehand, second the index, n (eq. 3) of a close-by comb line is determined using a wavelength meter, and then the beat frequency of the cw laser and the comb line is determined to provide the precise offset from the previously determined comb line index.

Alternatively, a cw laser can be locked to a frequency comb by forming a beat between the laser and a frequency comb tooth. This beat can then be phase locked to an RF reference that determines the offset between the frequency comb line and the cw laser frequency. This establishes an optical phase locked loop (OPLL) between the cw laser and the comb. To achieve a phase lock, sufficient bandwidth is required. Adequate bandwidth is typically given in the case of external cavity diode lasers (ECDL) via feedback to the injection current.

5 Noise considerations with a frequency comb

The noise properties of an optical frequency comb can be understood in terms of the elastic tape model (ETM) [20]. The elastic tape model is based on the fundamen-

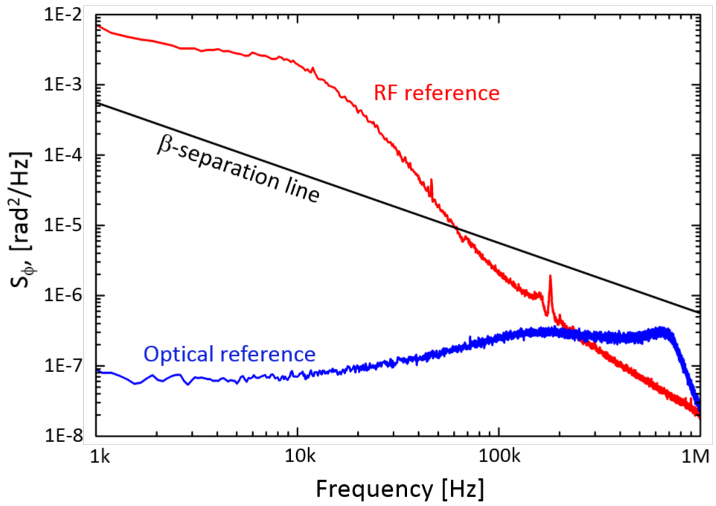

Figure 4. Phase noise measurements of the DFG frequency comb at 1162 nm with the comb locked to an RF reference (red) and a narrow line-width optical reference (blue). When locked to the optical reference, a Hz-level linewidth of the comb lines is achieved. The β-separation line (black) is shown for reference.

tal formula for the frequency of a comb line (eq. 3) and the assumption of linearly correlated changes in f_{rep} and f_{ceo} [21]. As an intuitive picture the comb breathes with like equidistant ticks on an elastic-tape that stays fixed at the fix point. For the type of Er:fibre oscillators used in frequency combs the observed fix-point for pump current modulation is at optical frequencies close to its emission spectrum [22]. By characterizing the noise properties of individual comb teeth it can be shown that the fix point of the DFG comb is, to a very good approximation, at the frequency origin [23]. Hence, the f_{rep} noise measured at one frequency can be rescaled to give the properties at any comb line. The phase noise of individual comb teeth at different wavelengths can be characterised by a beat with a narrow linewidth laser or, alternatively, by transferring the noise properties to an optically phase-locked (OPL) cw laser. The cw laser can subsequently be characterised using a delayed self-heterodyne (DSH) beat note [24].

Phase noise measurements of our DFG comb made at 1162 nm are shown in Fig. 4. The elastic tape model implies that the noise performance of the RF reference used to define the repetition rate will dominate the performance of the comb at optical frequencies, due to the 10^6 scaling given by the comb order, n. In fact, above a certain RF carrier offset frequency, typically on the order of 10 kHz, the optical oscillator is less noisy than the RF reference such that the performance of a frequency comb is related to the intrinsic noise properties of the oscillator, as evidenced by the corner 10 kHz frequency in Fig. 4. Much improved noise performance can be achieved by locking f_{rep} to an optical reference [23,25]. This greatly enhances the sensitivity of detection and improves the signal to noise ratio (SNR). The repetition rate can be phase locked to a narrow linewidth laser by creating an optical PLL where the phase error signal is generated from a beat between the narrow linewidth laser and a frequency comb tooth. In the case of the DFG comb, locking f_{rep} will provide a fully stabilised optical comb spectrum. When locked to a narrow linewidth optical reference, e.g., a diode laser locked to a high-finesse cavity, it is possible to simultaneously achieve Hz-level linewidth for all comb lines. Fig. 4 plots the phase noise of a DFG

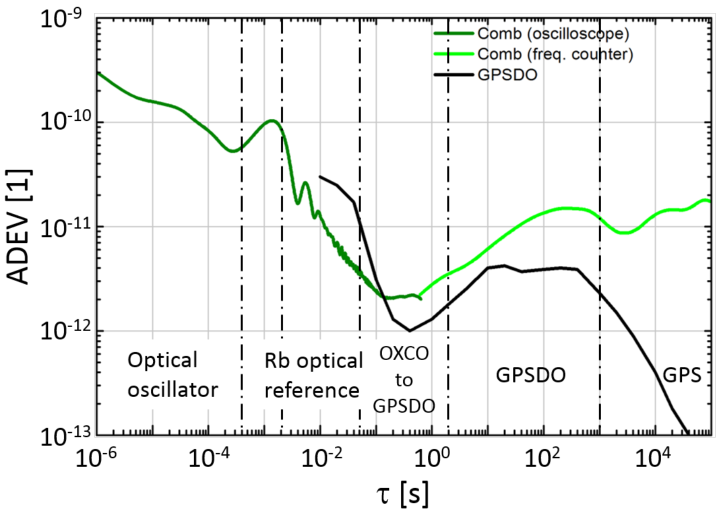

Figure 5. Allan deviation (ADEV) of the comb measured against Rb spectroscopy. The repetition rate $f_{\rm rep}$ is locked to an RF reference at the 10th harmonic at 800 MHz. The Allan deviation of the commercial oven-controlled crystal oscillator (OXCO) based GPS-disciplined RF reference (GPSDO) is shown for reference. The increase of the Allan deviation on long time scales is attributed to drifts in Rb spectroscopy. Note, that an oscillator with lower intrinsic noise shows lower ADEV at short time scales.

frequency comb locked to both an RF reference and a narrow line-width optical reference, showing the dramatic noise improvements that are possible when locking to an optical reference. The linewidth of the comb lines were on the Hz level when locked to the optical reference, compared to linewidth on the order of 100 kHz (integrated over 1-100 kHz) when locked to a low-noise RF reference. The β-separation lines provides a simple concept to the relation between noise and linewidth [26]. It has proven to be a good approximation for a large range of experimentally observed noise spectra. The power of an optical line is typically distributed between the optical carrier and a broader spectral background; the pedestal. The noise in frequency ranges exceeding the β-separation line contribute to the carrier linewidth, while the noise below the β-separation line contributes to the pedestal [27]. Hence, in the case of locking to an optical reference there is no contribution to the carrier width in the frequency range shown in Fig. 4.

The long term stability of the comb is characterised by the Allan deviation (ADEV). The ADEV is the standard deviation of the normalised frequency variations for a range of measurement intervals, τ [28] where the normalisation leads to unitless values. At short time scales the Allan deviation is calculated from the recorded beat and for longer times it is recorded by a zero-dead-time frequency counter. Fig. 5 shows the long term stability as an ADEV measured against Doppler-free saturation spectroscopy of Rb. Distinct limiting contributions can be identified at various time scales corresponding to the different locking stages. At short time scales the ADEV is limited by the oscillator noise, within the locking bandwidth it is limited by the Rb reference then by the lock to the ultra-low-noise reference oscillator, which in turn is locked to 10 MHz reference finally by the GPS. In this case the limit to the GPS cannot be observed because the local reference given by the Rb spectroscopy drifts, thus limiting the measured ADEV at long time scales.

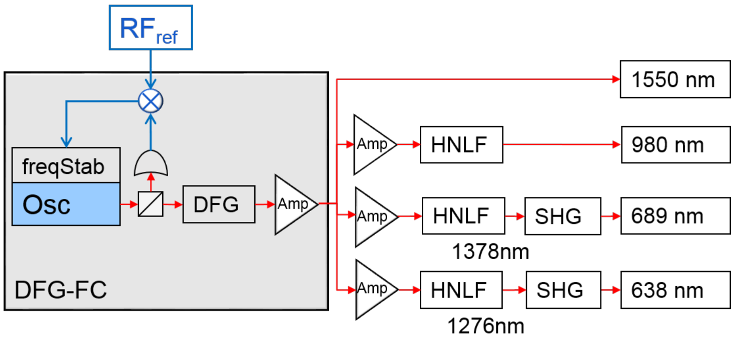

Figure 6. Frequency comb setup: The difference frequency comb (DFG-FC) delivers an $f_{\rm ceo}$-free spectrum that can be locked to an RF reference providing an absolutely stable frequency comb. The stable frequency comb can subsequently be converted by a highly-nonlinear fibre (HNLF) and/or second harmonic generation (SHG) to the desired wavelength outputs.

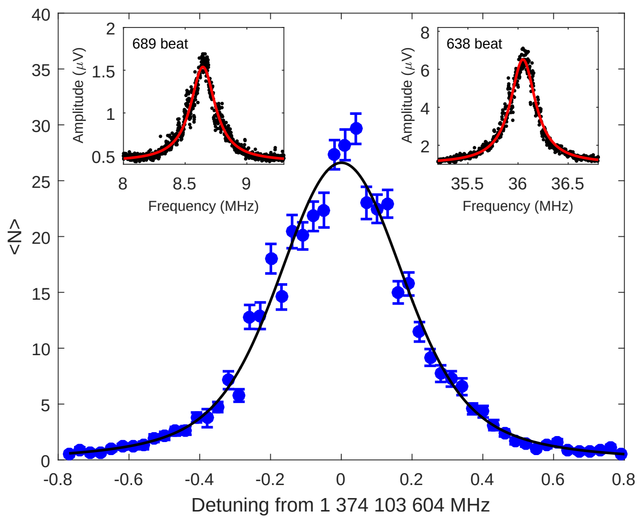

Figure 7. Precision Rydberg spectroscopy with the frequency comb. Insets show beat signals between the comb and the cw excitation lasers at 689 nm and 638 nm. Rydberg atoms are excited, ionised and detected in a cold cloud of Sr atoms as described in [6]. Using the measured beat frequencies, we obtain a plot of the ion signal $<N>$ versus the absolute frequency of the (^{88}Sr ^{1}S$_0 \rightarrow 5s37s\ ^3$S$_1, m_J = -1$) transition in a 3.1 G magnetic field (blue points). Black curve indicates a Gaussian fit to the spectrum.

6 An example application: precision spectroscopy of Sr Rydberg states

Precision spectroscopy of Rydberg states can be significantly improved by measuring against a frequency comb. In strontium, one possible excitation scheme for triplet Rydberg states requires 689 nm and a tunable source at 319 nm [6,29], these wavelengths have been used to access Rydberg states with principal quantum numbers $n = 24 - 81$ [6,29,30]. In [6] the UV light is generated by second harmonic generation (SHG) of 638 nm, hence precision Sr Rydberg spectroscopy requires frequency comb outputs at both 638 nm and 689 nm, see Fig. 6. The procedure for obtaining the Rydberg excitation spectrum is described in detail in [6]. Briefly, a laser cooled cloud of Sr atoms is illuminated with pulses of light at 689 nm and 319 nm, leading to the excitation of Rydberg atoms. Both lasers are independently stabilised to a high-finesse reference cavity and atomic spectroscopy lock. The Rydberg atoms are subsequently ionised, and the ions are counted electronically. To obtain the spectrum, the frequency of the UV laser is stepped precisely across the resonance. For the absolute measurement of the frequency at each step, the beat between each laser and a nearby comb line is detected with a photodiode. An example of the measured beat notes, and a Rydberg excitation spectrum with the resulting absolute frequency axis are shown in Fig. 7. Note that since the beat frequency is averaged, the frequency axis calibration is not limited by the short-term linewidth of the beat signal shown in Fig. 7.

The linewidth is limited by residual Doppler broadening [6] which is significant even at low temperatures due to the large wavevector of the UV light. By optimising the laser cooling, this can be reduced by a further factor of 3. Nevertheless, using a least squares fit the absolute frequency of the Rydberg line centre is determined with a statistical uncertainty of just 4 kHz, which is 3 orders of magnitude better than previous measurements [31]. Systematic frequency shifts due to magnetic and electric fields and the blackbody environment affect the line position, and the next challenge is to control these at a similar level. For the data shown in Fig. 7, our preliminary estimates suggest that these shifts are less than 1 MHz.

7 Conclusion

Frequency combs have great potential as general purpose tools for high precision measurements of optical frequencies as well as timing applications. In recent years significant scientific and technological advancements have been made both in the noise properties as well as in terms of versatility and integration. Applications require control of both parameters ($f_{\mathrm{ceo}}, f_{\mathrm{rep}}$) of the comb spectrum. In DFG combs the carrier envelope phase is fundamentally eliminated, removing the limitations of a feed-back-loop stabilisation. This provides for simpler comb operation making it a convenient tool to both accurately stabilise laser sources and accurately measure optical frequencies in Rydberg experiments and more generally in cold atom optics. Moreover, oscillator pump current is still available as a fast actuator for other purposes. This allows for a compact and robust, passively stable frequency comb solution. The increasing availability of frequency combs as laboratory tools open this potential to a wide range of precision measurements, in particular in cold atom physics.

NH and RK acknowledge support by Initial Training Networks QTea and COHERENCE, funded by the FP7 Marie Curie Actions of the European Commission ITN-317485 and ITN-265031, respectively.

Durham University acknowledge support from EPSRC grant EP/J007021/ and EU grants FP7-ICT-2013-612862-HAIRS and H2020-FETPROACT-2014-640378-RYSQ. Some research data supporting this paper is available at *link added later*; the remainder is commercially relevant but may be obtained under agreement by contacting the authors.

References

1. S.T. Cundiff and J. Ye, *Rev. Mod. Phys.* **75**, (2003) 325–342.
2. S.A. Diddams, *J. Opt. Soc. Am. B* **11**, (2010) B51.

3. A. Bartels, S.A. Diddams, C.W. Oates, G. Wilpers, J.C. Bergquist, W.H. Oskay, and L Hollberg, *Opt. Lett.* **30**, (2005) 667–669.
4. A. D. Ludlow, M. M. Boyd, J. Ye, E. Peik, and P. O. Schmidt, *Rev. Mod. Phys.* **87**, (2015) 637–701.
5. N. Poli, C.W. Oates, P. Gill, and G.M. Tino,*La Rivista del Nuovo Cimento* **36**, (2013) 555–624.
6. E.M. Bridge, N.C. Keegan, A.D. Bounds, D. Boddy, D.P. Sadler, and M.P.A. Jones, *Opt. Express* **24**, (2016) 2281–2292.
7. A. Kumar, P.K. Molony, P.D. Gregory, C.L. Blackley, C.R. Le Sueur, J. Aldegunde, J.M. Hutson, and S.L. Cornish. *ChemPhysChem.*, (2016) *Accepted*.
8. S. Rausch, T. Binhammer, A. Harth, J. Kim, R. Ell, F.X. Kärtner, and U. Morgner, *Opt. Express* **16**, (2008) 9739–9745.
9. L. Xu, G. Tempea, A. Poppe, M. Lenzner, Ch. Spielmann, F. Krausz, A. Stingl, and K. Ferencz, *Appl. Phys. B* **65**, (1997) 151–159.
10. A. Sell, G. Krauss, R. Scheu, R. Huber, and A. Leitenstorfer, *Opt. Express* **17**, (2009) 1070–1077.
11. K Tamura, E.P. Ippen, H.A. Haus, and L.E. Nelson, *Opt. Lett.* **18**, (1993) 1080–1082.
12. D.J. Jones, S.A. Diddams, J.K. Ranka, A. Stentz, R.S. Windeler, J.L. Hall, and S.T. Cundiff, *Science* **288**, (2000) 635–639.
13. S. Koke, Ch. Grebing, H. Frei, A. Anderson, A. Assion, and G. Steinmeyer, *Nature Photon.* **4**, (2010) 462–465.
14. T. Fuji, A. Apolonski, and F. Krausz, *Opt. Lett.* **29**, (2004) 632–634.
15. M. Zimmermann, Ch. Gohle, R. Holzwarth, T. Udem, and T.W. Hänsch, *Opt. Lett.* **29**, (2014) 310–312.
16. D. Fehrenbacher, P. Sulzer, A. Liehl, T. Kälberer, C. Riek, D.V. Seletskiy, and A. Leitenstorfer, *Optica* **2**, (2015) 917–923.
17. G. Krauss, D. Fehrenbacher, D. Brida, C. Riek, A. Sell, R. Huber, and A. Leitenstorfer,*Opt. Lett.* **36**, (2011) 540–542.
18. V. Dolgovskiy, N. Bucalovic, P. Thomann, Ch. Schori, G. Di Domenico, and S. Schilt, *J. Opt. Soc. Am. B* **29**, (2010) 2944–2957.
19. W. Zhang, M. Lours, M. Fischer, R. Holzwarth, G. Santarelli, and Y. Le Coq, *IEEE Transactions on Ultrasonics, Ferroelectrics, and Frequency Control* **50**, (2012) 432–438.
20. H.R. Telle, B. Lipphardt, and J. Stenger, *Appl. Phys. B* **74**, (2002) 1–6.
21. E. Benkler, H.R. Telle, A. Zach, and F. Tauser, *Opt. Express* **13**, (2005) 327–332.
22. N. Haverkamp, H. Hundertmark, C. Fallnich, and H.R. Telle, *Appl. Phys. B* **78**, (2004) 321–324.
23. T. Puppe, A. Sell, R. Kliese, N. Hoghoogi, A. Zach and W. Kaenders, *Opt. Lett.* **41**, (2016) 1877-1880.
24. T. Okoshi, K. Kikuchi, and A. Nakayama, *Electron. Lett.* **16**, (1980) 630–631.
25. A. Bartels, S.A. Diddams, T.M. Ramond, and L. Hollberg, *Opt. Lett.* **28**, (2003) 663–665.
26. G. Di Domenico, S. Schilt, and P. Thomann, *Appl. Opt.* **49**, (2010) 4801–4807.
27. N. Bucalovic, V. Dolgovskiy, Ch. Schori, P. Thomann, G. Di Domenico, and S. Schilt, *Appl. Opt.* **51**, (2012) 4582–4588.
28. D. W. Allan, *Proceedings of the IEEE* **54.2** (1966) 221–230.
29. B.J. DeSalvo, J.A. Aman, C. Gaul, T. Pohl, S. Yoshida, J. Burgdörfer, K.R.A. Hazzard, F.B. Dunning, and T.C. Killian, *Phys. Rev. A* **93**, (2016) 022709.
30. B.J. DeSalvo, J.A. Aman, F.B. Dunning, T.C. Killian, H.R. Sadeghpour, S. Yoshida, and J. Burgdörfer, *Phys. Rev. A* **92**, (2015) 031403.
31. R. Beigang, K. Lücke, A. Timmermann, P.J. West, and D. Frölich, *Opt. Commun.* **42**, (1982) 19–24.